Available online at www.sciencedirect.com
ScienceDirect
Ceramics International 33 (2007) 1375–1379
CERAMICS INTERNATIONAL
www.elsevier.com/locate/ceramint

Nucleation of lithium aluminosilicate glass containing complex nucleation agent

Xingzhong Guo *, Hui Yang, Chen Han, Fangfang Song

Center for Nano-Science and Nano-Technology of Zhejiang University, Hangzhou 310027, China

Received 20 February 2006; received in revised form 9 March 2006; accepted 28 April 2006
Available online 11 September 2006

Abstract

The nucleation behavior of lithium aluminosilicate (Li_2O–Al_2O_3–SiO_2, LAS) glass containing complex nucleation agent (TiO_2 + Z-rO_2 + P_2O_5+/or F^-) were investigated by the differential thermal analysis (DTA), X-ray diffraction (XRD), transmission electron microscopy (TEM) and infrared (IR) spectroscopy. DTA of annealed glass showed that the addition of P_2O_5 obviously increased the transition temperature (T_g) while the addition of F^- decreased it, and both P_2O_5 and F^- decreased the temperatures (T_p) and the amount of crystallization peaks. DTA of pre-nucleated glass showed that the suitable nucleating system of the LAS glass containing P_2O_5 was 740 °C/1.5 h, but 700 °C/1.0 h for that containing both P_2O_5 and F^-, both were higher than that containing no P_2O_5. XRD of nucleated glass showed that two nucleation phases ($LiAl(SiO_3)_2$ and $LiAlSi_3O_8$) formed and co-existed above the suitable nucleation temperature, and the formation temperature of nucleation phases for sample containing P_2O_5 was higher than that containing both P_2O_5 and F^-, which coincided with the DTA results and was also confirmed by the IR and TEM analysis. The complex nucleation agent can improve the nucleation of LAS glass by F^--decreasing nucleation temperature and time and P_2O_5-increasing the amount of nuclei.

Keywords: D. Glass; Li_2O–Al_2O_3–SiO_2; Nucleation; Complex nucleation agent

1. Introduction

The lithium aluminosilicate (Li_2O–Al_2O_3–SiO_2, LAS) system glass ceramic has been widely studied and used in many fields because of its low thermal expansion coefficient, high thermal shock resistance and long chemical durability [1–3]. Proper nucleation agents in the composition of the initial glass and adequate thermal treatment are the crucial issues in obtaining high quality and low cost glass ceramic [4–6]. The most popular nucleation agents of LAS glass are TiO_2, ZrO_2, etc., and fluorine (F) has recently been introduced as a nucleation agent to accelerate the nucleation and crystallization of LAS glass [7,8]. P_2O_5 has also been used as a nucleation agent in a wide category of glass ceramic including Li_2O–SiO_2, Li_2O–Al_2O_3–SiO_2, Li_2O–MgO–SiO_2, MgO–Al_2O_3–SiO_2 [9,10] and apatite glass ceramics [11].

The nucleation stage is very important in controlling the crystallization and obtaining a fine microstructure [5]. Riello et al. [2] studied the nucleation behavior of LAS glass ceramic by determining the nucleation phase and its concentration. Bengisu and Brow [12] performed a long-term heating and thermal cycling of LAS glass ceramic and found that low temperature nucleation had more advantages than high temperature nucleation. The present studies on the nucleation stage of LAS glass ceramic focuses on the effect of nucleation on the crystallization, properties and microstructure of the glass ceramic.

The complex nucleation agent consisting of TiO_2, ZrO_2, P_2O_5 and/or F^- were used in the LAS system, and the nucleation behavior of LAS glass containing complex nucleation agent were monitored and analysed by DTA, XRD, IR and TEM.

2. Experimental

2.1. Glass preparation

Acid washed quartz sands and chemical reagents of high purity Li_2CO_3, Al_2O_3, MgO, ZnO, ZrO_2, TiO_2, P_2O_5, F^- and other additions were used to produce the glass batches. The compositions of all batches were listed in Table 1, in which the

* Corresponding author. Tel.: +86 571 87953313; fax: +86 57187953054.
E-mail address: gxzh_zju@163.com (X. Guo).

0272-8842/$32.00
doi:10.1016/j.ceramint.2006.04.019

Table 1
Main compositions of the glass batches (wt%)

Compositions	G-0 [8]	G-F [8]	G-P	G-PF
Li_2O	3.5	3.5	4.0	4.0
Al_2O_3	19.8	19.8	19.5	19.5
SiO_2	67.5	67.5	67	67
ZnO + MgO + BaO	1.8	1.9	1.7	1.7
$Na_2O + K_2O$	2.2	2.2	2.0	2.0
$TiO_2 + ZrO_2$	5.2	4.0	4.5	4.0
F^-	–	0.8	–	0.5
P_2O_5	–	–	0.5	0.5

G-0 and G-F samples are provided by our previous studies [8]. Each glass batch was melted for 3–6 h at 1550–1620 °C, stirred to encourage homogeneity and moulded in a pre-heated die. The glass was annealed at 580 °C for 1 h to eliminate internal stress.

2.2. Nucleation

The glass samples were pre-nucleated at 640–820 °C (every 20 °C) for 1 h with a heating rate of 20 °C/min. Subsequently, the pre-nucleated samples were fast-cooled, ground and sieved through a 200-mesh screen to obtain the glass powder. A differential thermal analyzer (NETZSCH STA 409 PC Luxx, Germany) with a heating rate of 20 °C/min was used to study the differential thermal analysis (DTA) of the glass powders. According to the crystallizing peak temperatures (T_p, temperature at main exothermic peak of DTA curve) at different pre-nucleation temperatures and time, the suitable nucleation temperature and time can be obtained.

2.3. Characterization

The thermal behavior of the annealed glasses was also performed by using differential thermal analysis. Powder X-ray diffraction (XRD) was used to identify the nucleation phases in the materials before and after nucleation. Powder sample were prepared from bulk materials by crushing in a percussion mortar. A XJ10-60 X-ray diffractometer was used with nickel filtered Cu Kα radiation, and the scan range from 10 to 80°, at a step of 0.02° and at a scanning speed of 2° min^{-1}. Infrared (IR) transmittance spectra of the glass samples were measured by using the standard KBr-pellet technique with an infrared analyzer (AVATAR 360FT Nicolet). The microstructure of the nucleated glass was observed by transmission electron microscopy (TEM, model: Jeol JEM-200CX).

3. Results and discussions

3.1. DTA of annealed glass

Fig. 1 shows the DTA traces obtained from annealed G-P and G-PF glass powders. The glass transition temperatures (T_g) and crystallization temperature (T_p) of all glass samples are picked up and listed in Table 2. T_g for the glass samples

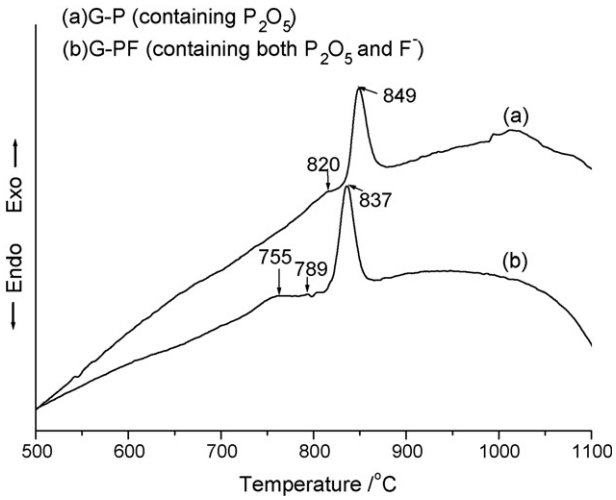

Fig. 1. DTA traces obtained from G-P and G-PF glass powders.

containing P_2O_5 (G-P, $T_g \approx 820$ °C and G-PF, $T_g \approx 755$ °C) are 200–300 °C higher than that for the samples without P_2O_5 (G-0, $T_g \approx 532$ °C and G-F, $T_g \approx 520$ °C), and T_g for glass samples containing F^- (G-F and G-PF) are lower than that for samples without F^- (G-0 and G-P). These suggest that P^{5+} (network forming ion) enhances the transition temperature while F^- (network modifying ion) reduces it. The sample free of P_2O_5 and F^- exhibits five crystallization peaks with a prominent peak of 860 °C, higher than the corresponding peaks of the samples containing P_2O_5 and/or F^- respectively. Only one crystallization peak (849 °C) is found in the samples containing P_2O_5 and the prominent peak (837 °C) of the sample containing both P_2O_5 and F^- is the lowest. It may be concluded that both P_2O_5 and F^- can promote the crystallization of the LAS glass.

3.2. Nucleation of annealed glass

The DTA analysis is regarded as a relatively exact method to determine the nucleation temperature and time of glass. Due to many nuclei with a nanometer size having formed in pre-nucleation process, crystallization mainly involving grain growth starts at a relatively low temperature, which is confirmed by the fact that T_p shifts to a lower temperature in DTA system. Therefore, the shift of crystallization temperature may be used to study the nucleation process of LAS glass.

Fig. 2 shows the DTA traces of G-P and G-PF glasses after pre-nucleated. It is noted that the pre-nucleation temperature

Table 2
Glass transition and crystallization temperatures

	T_g (°C)	Crystallization peaks (°C)				
G-0 [8]	532	690	710	760	810	860 (P)[a]
G-F [8]	520	685		760	810	844 (P)
G-P	820					849 (P)
G-PF	755			789	809	837 (P)

[a] (P) indicates a prominent peak.

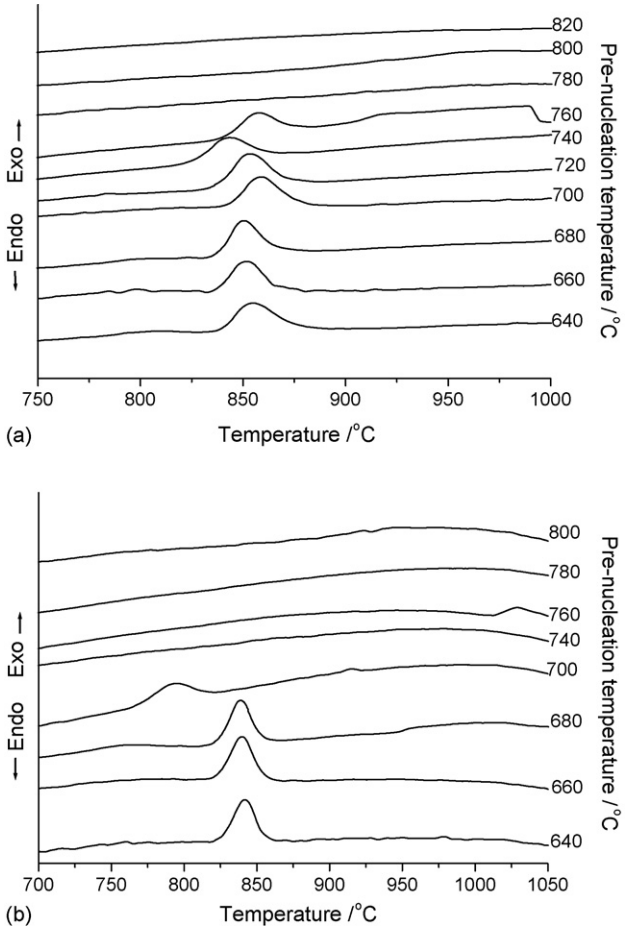

Fig. 2. DTA trace of the glass after pre-nucleated at different temperatures (a) G-P (containing P_2O_5); (b) G-PF (containing both P_2O_5 and F^-).

has an influence on T_p, which is summarized in Fig. 3. With the increase of pre-nucleation temperature, the T_p first decreases, becomes the lowest at the pre-nucleation temperature of 740 °C for G-P sample (700 °C for G-PF sample), and then increases rapidly. It indicates that the suitable nucleation

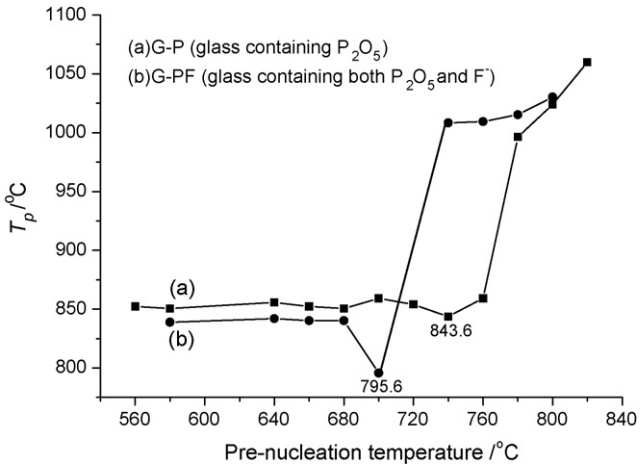

Fig. 3. Relationship between crystallization peak temperatures and pre-nucleation temperatures.

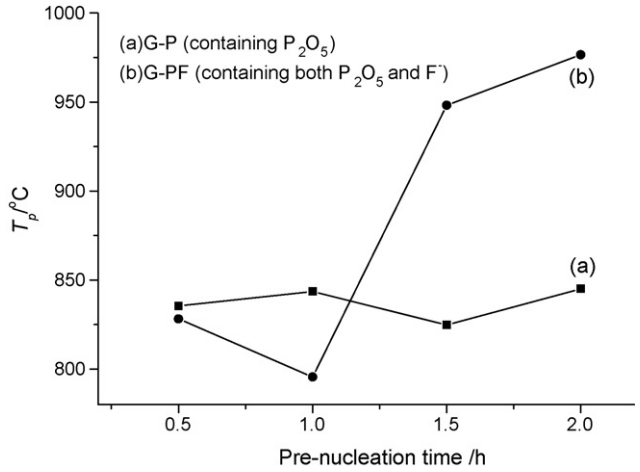

Fig. 4. Relationship between crystallization peak temperatures and pre-nucleation times at a suitable nucleation temperature (G-P: 740 °C; G-PF: 700 °C).

temperatures of G-P and G-PF samples are 740 and 700 °C, respectively. The nucleation temperature of G-0 and G-F glasses is 660 and 620 °C, respectively [8], which confirms that the addition of P_2O_5 increases the nucleation temperature by 40–120 °C, while the addition of F^- decreases it by 40–60 °C. Above the suitable nucleation temperature, the nuclei merge and the amount of nuclei reduce, resulting in the T_p shifting to higher [5].

The nucleation time of LAS system glass ceramic determines the amount and growth of nuclei in nucleation stage, and affects the crystallization in the subsequent heat treatment and finally the microstructure and properties of glass ceramic [13]. By changing pre-nucleation time at certain pre-nucleation temperature, the crystallization peak temperature was further studied using by DTA analysis. Fig. 4 shows the relationship between the crystallization peak temperatures (T_p) and pre-nucleation time at the suitable nucleation temperature. For G-PF curve T_p decreases with the pre-nucleation time, becomes the lowest at 1 h, and then increases rapidly again, which indicates that the suitable nucleation time is 1 h for G-PF sample (containing P_2O_5 and F^-). With the same method, the suitable nucleation time for G-P sample (containing P_2O_5) is 1.5 h due to the G-P curve, 0.5 h longer than that for G-PF sample, which confirms that fluorine can promote the nucleation of glass by decreasing the nucleation temperature and time.

3.3. XRD analysis of nucleated glass

Present researches pay little attention to nucleation phases in nucleation stage of glass. Actually, the nucleation phase analyses can tell whether the heat treatment is dominated by further nuclear formation or by nuclei growth. The XRD patterns of G-P and G-PF glasses after nucleated at 740 °C/1.5 h and 700 °C/1 h are shown in Fig. 5. It can be seen that G-P samples nucleated at and below 760 °C are amorphous. The sample nucleated at 800 °C is found to have nucleation phases of tetragonal $LiAlSi_3O_8$ (JCPDS 35-0794) and hexagonal $LiAl(SiO_3)_2$ (31-0706). For G-PF samples, two coexisting

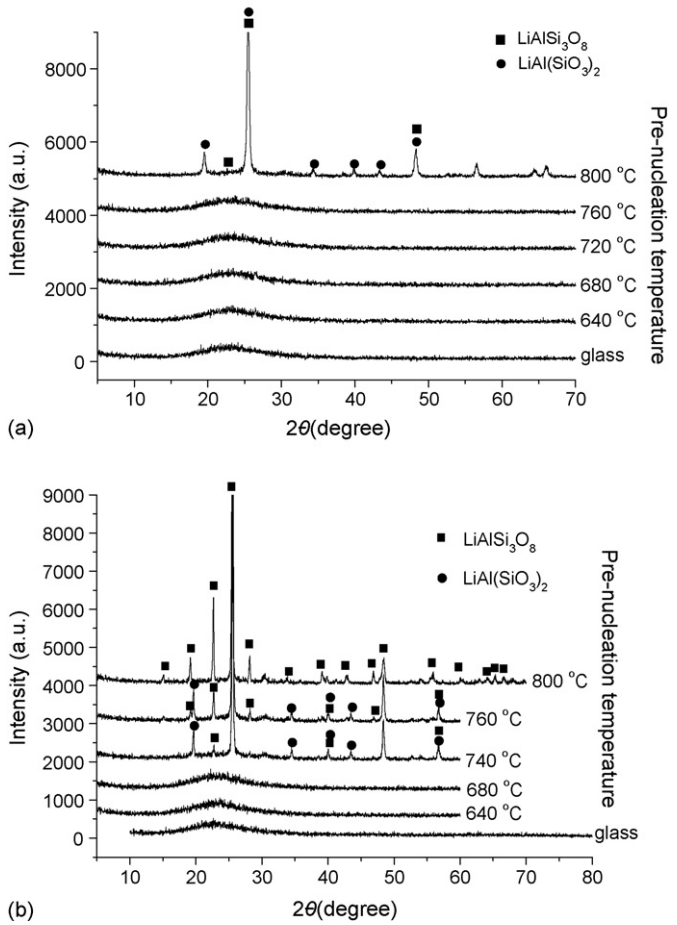

Fig. 5. XRD patterns of G-P and G-PF glasses after nucleation: (a) containing P_2O_5; (b) containing both P_2O_5 and F^-.

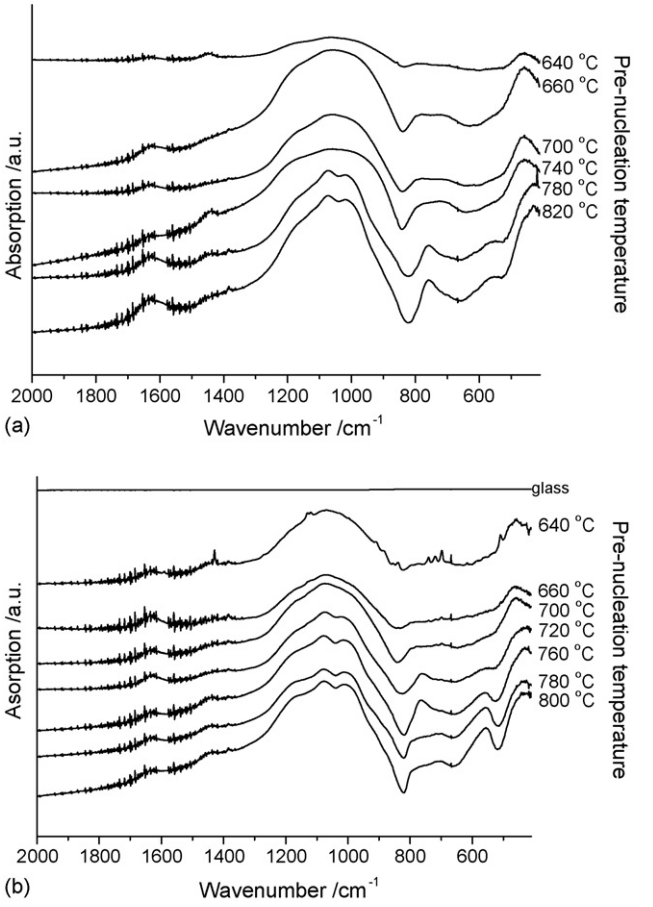

Fig. 6. IR spectra of G-P and G-PF glasses after nucleation: (a) containing P_2O_5; (b) containing both P_2O_5 and F^-.

crystalline phase (tetragonal $LiAlSi_3O_8$ and hexagonal $LiAl(SiO_3)_2$) are observed in those pre-nucleated at 740 °C and 760 °C, and single phase of tetragonal $LiAlSi_3O_8$ exists in that pre-nucleated at 800 °C.

The nucleation of glass usually aims at the highest nuclear density, rather than nucleation phase. According to the XRD results, the suitable nucleation temperatures should be considered below 800 and 740 °C for the G-P and G-PF glasses respectively, which are in agreement with the results by DTA.

3.4. IR spectra of nucleated glass

The IR absorption spectrum of each glass in this study has its own characteristic shape. The main peaks are directly connected with the bands present in the polycrystalline phases [14]. We will utilize the IR spectra to study the structure of glass in the nucleation stage.

Fig. 6 shows the IR spectra of G-P and G-PF glasses after pre-nucleation. Two major absorption bands at ∼1050 and 480 cm^{-1} are found in the IR spectra of G-P nucleated glass. With the increase in nucleation temperature, the ∼1050 cm^{-1} band becomes broader and higher, the 480 cm^{-1} band shifts to lower wave number (to ∼450 cm^{-1} for the sample at 820 °C), and two weak shoulders at ∼1070 and 760 cm^{-1} occur for the sample pre-nucleated at 780 °C and above, indicating the new phase generation or phase transformation. Dissimilar to that of G-P sample, G-PF nucleated glass exhibits two weak shoulders at ∼1010 and 760 cm^{-1} only after pre-nucleated at 720 °C and above. The IR spectra confirm that the addition of P_2O_5 can increase the formation temperature of new phase, while the addition of F^- works reversely.

3.5. TEM observation of nucleated glass

Fig. 7 shows TEM bright field images of G-P and G-PF nucleated samples. The microstructure is characterised by spherical nuclei 20–50 nm in diameter. The G-PF nucleated sample has a higher nuclei concentration and a smaller particle size than those of G-P sample. Electron diffraction pattern of G-P nucleated sample shows tetragonal crystalline structure (possibly tetragonal $LiAlSi_3O_8$) with more diffraction rings, but mixed crystalline structure with more diffraction rings for G-PF nucleated sample, which possibly consists of tetragonal $LiAlSi_3O_8$ and hexagonal $LiAl(SiO_3)_2$ according to the above results of XRD.

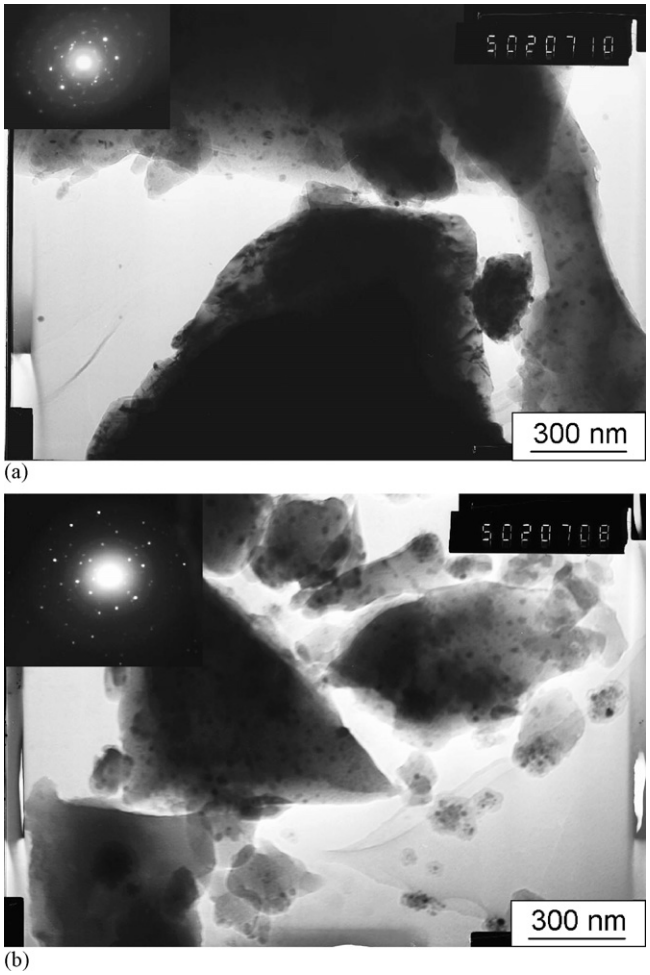

(a)

(b)

Fig. 7. TEM images of nucleated glasses: (a) containing P_2O_5; (b) containing both P_2O_5 and F^-.

4. Conclusions

This research aimed at investigating the nucleation behavior of Li_2O–Al_2O_3–SiO_2 system glass ceramic containing complex nucleation agent by employing DTA, XRD, IR and TEM techniques. This study had succeeded in obtaining the nucleation characteristics of LAS system glass containing complex nucleation agents. As a result, the suitable nucleation system of glass containing P_2O_5 was 740 °C/1.5 h, and 700 °C/1.0 h for glass containing P_2O_5 and F^-, both were higher than that containing no P_2O_5. The nucleation phases during the nucleation stage were tetragonal $LiAlSi_3O_8$ and hexagonal $LiAl(SiO_3)_2$, became sole $LiAlSi_3O_8$ with the increase of nucleation temperature, accompanied with a nuclei size of 20–50 nm. The complex nucleation agent can improve the nucleation of the glass by F^--decreasing nucleation temperature and time and P_2O_5-increasing the amount of nuclei.

Acknowledgement

This work is supported by the High Science & Technique Brainstorm Project (no. 2003C11030) of Zhejiang Province of China.

References

[1] M. Guedes, A.C. Ferro, J.M.F. Ferreira, Nucleation and crystal growth in commercial LAS compositions, J. Euro. Ceram. Soc. 21 (2001) 1187–1194.
[2] P. Riello, P. Canton, N. Comelato, Nucleation and crystallization behavior of glass–ceramic materials in the Li_2O–Al_2O_3–SiO_2 system of interest for their transparency properties, J Non-Cryst. Solids 288 (2001) 127–139.
[3] P.F. James, Glass ceramics: new compositions and uses, J Non-Cryst. Solids 181 (1995) 1–15.
[4] J.H. Perepezko, Nucleation-controlled reactions and metastable structure, Prog. Mater. Sci. 49 (2004) 263–284.
[5] P.W. Mcmilan, Glass Ceramics, Academic Press, 1979.
[6] A.M. Hu, K.M. Liang, F. Zhou, G.L. Wang, Phase transformations of Li_2O–Al_2O_3–SiO_2 glasses with CeO_2 addition, Ceram. Int. 31 (2005) 11–14.
[7] A.M. Hu, K.M. Liang, F. Peng, Crystallization and microstructure changes in fluorine-containing Li_2O–Al_2O_3–SiO_2 glasses, Thermochim. Acta 413 (2004) 53–55.
[8] X.Z. Guo, H. Yang, M. Cao, Nucleation and crystallization behavior of Li_2O–Al_2O_3–SiO_2 system glass–ceramic containing little fluorine and no-fluorine, J. Non-Cryst. Solids 351 (2005) 2133–2137.
[9] U. Kang, T.I. Chuvaeva, A.A. Onushchenko, A.V. Shashkin, Radiative properties of Nd-doped transparent glass–ceramics in the lithium aluminosilicate system, J. Non-Cryst. Solids 278 (2000) 75–84.
[10] W. Höland, V. Rheinberger, M. Frank, Mechanisms of nucleation and controllied crystallization of needle-like apatite in glass–ceramics of the SiO_2–Al_2O_3–K_2O–CaO–P_2O_5 system, J. Non-Cryst. Solids 253 (1999) 170–177.
[11] S. Taruta, K. Mukoyama, S.S. Suzuki, Crystallization process and some properties of calcium mica–apatite glass–ceramics, J. Non-Cryst. Solids 296 (2001) 201–211.
[12] M. Bengisu, R.K. Brow, Effect of long-term heating and thermal cycling on thermal expansion, phase distribution, and microhardness of lithium aluminosilicate glass–ceramic, J. Non-Cryst. Solids 331 (2003) 137–144.
[13] J.R. Frade, C.M. Queiroz, M.H. Fernandes, Simulated effects of transient nucleation on the crystallization of glass samples, J. Non-Cryst. Solids 333 (2004) 263–271.
[14] M. Nocuń, M. Handke, Structural inhomogeneity in glasses from the system Li_2O–Al_2O_3–SiO_2 revealed by IR spectroscopy, J. Mol. Struct. 596 (2001) 139–143.